

ORIGINAL RESEARCH PAPER

## Ab initio (first principle) material modeling study on Lio adsorbed by palladium-cobalt (PdCo) nanoparticles

Mikail Aslan\*

Department of Metallurgical and Materials Engineering, Gaziantep University, Üniversite Bulvarı, Şehitkamil, Gaziantep, 27310, Turkey

Received: 2019-06-19

Accepted: 2019-06-19

Published: 2019-09-20

### ABSTRACT

PdCo subnanoalloys have been commonly used as a catalytic material in some important chemical reactions, involving in fisher-tropsch reactions, and oxygen reduction reactions. In terms of understanding the role of catalysis, these smallest bimetallic nanoparticles provide the simplest prototypes of Pd-Co bimetallic catalysts for different compositions. In this study, the effect of  $\text{Li}_x\text{O}$  ( $x=1,2$ ) on PdCo nanoalloys has been investigated comprehensively employing the density functional theory (DFT) to identify the mechanism of structural, electronic, and energetic properties of the studied species. Binding energies are calculated for stability analysis, which is very important for nanoparticles. Results show that lithium oxides are generally adsorbed by cobalt sites on the Pd-Co substrate. This is important for determining active sites of the catalytic material. Furthermore, the structures have low symmetric properties. Hence, this study might provide an initial structural evaluation step for future studies related to the possible new catalytic material of Li-air batteries.

**Keywords:** *Ab Initio Method; Bimetallic Nanoparticles; Catalytic Material; Clusters; Computational Material Modeling; DFT; Electronic Properties; First Principle; Nanoalloys; Nanomaterials; Nanoshaping; Stability*

© 2019 Published by Journal of Nanoanalysis.

### How to cite this article

Aslan M. *Ab initio (first principle) material modeling study on Lio adsorbed by palladium-cobalt (PdCo) nanoparticles*. J. Nanoanalysis., 2019; 6(4): 247-255. DOI: 10.22034/jna.\*\*\*

## INTRODUCTION

Nanoparticles (which range from 1 to 100 nm) can be classified as a new category of material class since they show very different properties from their conventional bulk materials. These properties lead to the current subject of intense investigation and research in many nanoscale applications, such as synthesis and catalysis of polymer[1], gas phase spectroscopy[2], biochemistry[3], magnetic recording media[4], medicine[5] and electronic devices [6], metal[7] and ceramic characterization[8] and catalysis[9-10]. Especially, they are used in catalysis. In the chemical industry, the study of bimetallic nanoalloys or nanoparticles (which are consist of two different

elements) catalysts are of greater interest than monometallic ones since their properties may be tuned by changing their compositions, sizes, and geometries. Furthermore, a catalytic activity of a species for a specific reaction is related to the local electronic environments of the catalytic material. Pure transition metal nanoalloys produce more significant charge localization than their bulk surfaces[11].

PdCo nanoalloys have been commonly referred to as catalysts in some important chemical reactions, involving in fisher-tropsch reactions[12-14], and oxygen reduction reaction (ORR) [15], PdCo nanoparticles form ordered patterns at low temperatures and Pd tends to segregate to the

\* Corresponding Author Email: [aslanm@gantep.edu.tr](mailto:aslanm@gantep.edu.tr)

surface in the case of macroscopic samples of PdCo bimetallic nanoalloys[16]. Furthermore, PdCo particles have shown improved selectivity over pure Co particles, Scientist and materials and chemical engineers have focused on the improvement of cost-advantage catalysts related to mixed transition metal oxides[17-19]. For the ORR reaction, Leng et al[20] studied catalysis based on highly dispersed PdM (M = Fe, Co, Ni) alloy nanoparticles for catalysts of Li-O<sub>2</sub> reaction. They found a new type of catalyst which shows excellent ORR activity. Sevim et al. [21] investigated the performance of bimetallic PtM (M: Co, Cu, Ni) alloy nanoparticles as cathode catalysts for lithium-oxygen (Li-O<sub>2</sub>). They found that alloying Pt with different metals leads to change the morphology of Li<sub>2</sub>O<sub>2</sub> product importantly, which affect the subsequent recharge process.

Using DFT that is an efficient technique for studying the properties of nanoscaled materials, for understanding the role of catalytic material in Li-O system, these smallest bimetallic nanoparticles provide the simplest prototypes of Pd-Co bimetallic catalysts. Thus, this study will provide initial, basic information of structural characterization for Pd-Co catalytic mechanism of Li-O to some extent.

## METHODOLOGY

The calculations are carried out in the framework of DFT with the generalized gradient approximation (GGA) of Becke's exchange functional [22] and Lee-Yang-Parr correlational functional[23] in the NWChem 6.0 package[24] which provides finding the lowest energetic structures and conducting structural characterization of materials. CRENBL [25] basis set for Pd and Co elements, including effective core potential and 6-311++G\*\* basis set for Li and O elements has been chosen. For NWChem calculations, we have employed convergence criteria as  $1 \times 10^{-6}$  Hartree for energy and  $5 \times 10^{-4}$  Hartree/a<sub>0</sub> for energy gradient. No symmetric constraints were imposed during geometrical optimizations using various electronic spin multiplies. Detail information about this method is given in Valiev's study[26]. Lastly, we have implemented the fully self-consistent vdW-DFT at the GGA level, with the Becke's exchange functional and Lee-Yang-Parr correlational functional. The exchange functional is favorable for calculating vdW interactions[27].

## RESULTS AND DISCUSSION

### Lowest Energy Structures of Pd<sub>n</sub>Co<sub>m</sub>LiO (2 ≤ n+m ≤ 4)

To check the validity of the computational method for the study of the bimetallic PdCoLiO nanoalloys, the bond length of Pd dimers was calculated as 2.40 Å. The obtained results are in agreement with experimental[28] (2.470 Å) and theoretical result[29] (2.48 Å). The lowest-lying energetic structures of Pd<sub>n</sub>Co<sub>m</sub>LiO (2 ≤ n+m ≤ 4) mixed metal oxides are shown in Fig. 1 and the density plots of the energy of the highest occupied molecular orbital (HOMO) and the energy of the lowest unoccupied molecular orbital (LUMO) calculations are given in Fig. 2.

Also, total spin moments, binding energies (BEs), fermi energies (FEs) and HOMO-LUMO Gaps (HLGs) of the studied nanoparticles are presented in Table 1. For each case in the present study, LiO is adsorbed on the PdCo nanoparticles molecularly with oxygen rather than lithium. When LiO molecule absorbed at PdCo surface, a top or bridge site is observed and in these complexes, LiO favors to bind Co atom. The most stable structure of Pd<sub>2</sub>LiO having Cs symmetry is in the quartet magnetic state with a Pd-Pd bond distance of 2.44 Å. The patterns of molecular orbitals demonstrated that PdCoLiO has similar bonding behaviours to those of Pd<sub>2</sub>LiO (see Fig. 2). The addition of Co atom instead of Pd atom causes a very little stretch in the Co-O bond length that has value of 1.75 Å. The BE of Co<sub>2</sub>LiO is the highest value among the species at size 2. For these structures, the BE increases when the ratio of Co/Pd increases.

In the lowest energy structure of Pd<sub>3</sub>LiO as shown in Fig. 1d, LiO is adsorbed as bridge site of the triangularly oriented Pd atoms. In comparison to the structure of Pd<sub>2</sub>LiO, the Li-O bond distance is stretched by 0.14 Å while the Pd-O bond distance is elongated as 0.1 Å. The average Pd-Pd bond distance of Pd<sub>3</sub>LiO is 2.73 Å. The magnetic spin moment of Pd<sub>3</sub>LiO is 1 μ<sub>B</sub>. The symmetry group is also C<sub>s</sub>. Its FE is found as 3.78 eV and the HLG is calculated as 0.50 eV. It's BE per atom is 2.36 eV (see Table 1). As one of the Pd atoms replaced with Co, the ground state of Pd<sub>2</sub>CoLiO structure becomes the structure having triangular bimetallic unit (consisting of a Co atom at the apex and two Pd atoms of the base). Replacement of Pd atom with Co atom has very little effect on Li-O bond length (1.83 Å), while it is 1.82 Å for Pd<sub>3</sub>LiO. The Pd-Pd bond distance is longer by 0.18 Å than that of Pd<sub>2</sub>LiO while the Pd-Co bond distances are 2.40 Å and 2.41 Å in

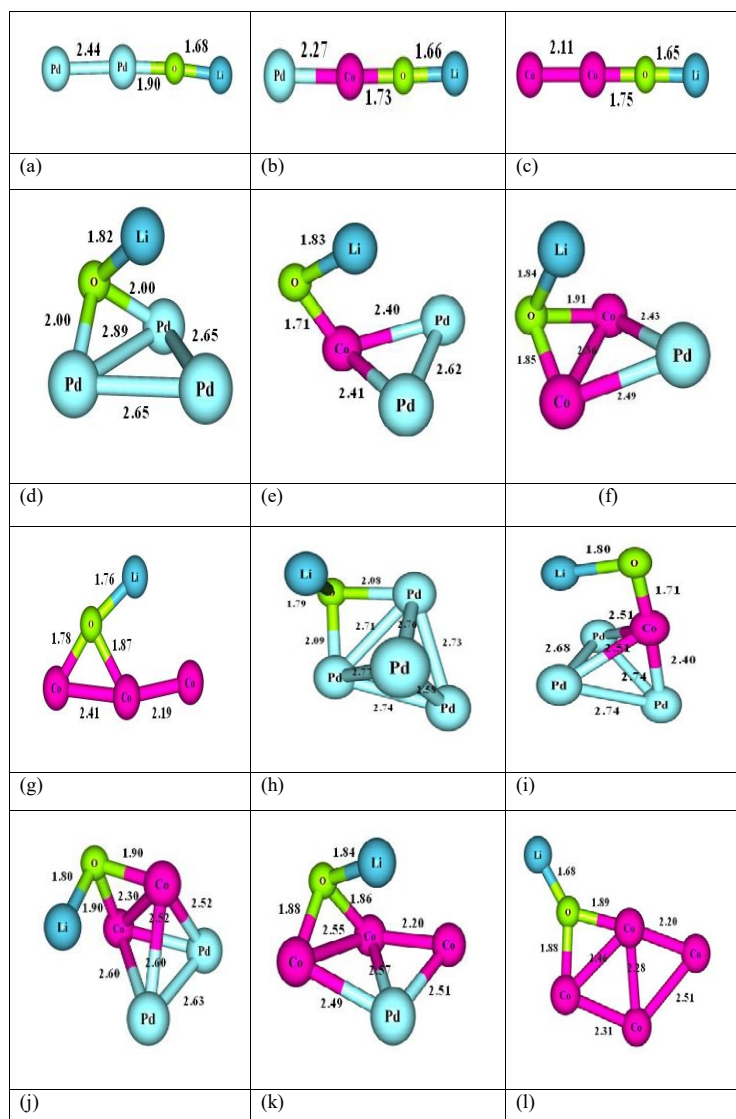


Fig. 1. The optimized structure of  $Pd_n Co_m LiO$  Nanoparticles ( $2 \leq m+n \leq 4$ )

$CoPd_2LiO$ . The FE is 0.17 eV, which is less than the FE of  $Pd_3LiO$ . The magnetic moment of  $Co_3LiO$  is septet. The Li-O bond distance becomes 1.76 Å when the LiO molecule is adsorbed on the bridge site whereas the value of the bond distance in the case of atop adsorption is 1.83 Å. These values can be compared to Li-O bond length of the free LiO molecule, which is calculated as 2.43 Å. This means that Li-O bond distance is shrunk notably upon the adsorption of the molecule on the Pd-Co nanoparticles.

The structure of  $Pd_4LiO$  complex has tetrahedral unit (see Fig. 1h) where the average Pd-Pd bond distance is 2.72 Å. The LiO is adsorbed on the bridge site for Pd tetramer, where the Pd-O distances are

2.08 Å and 2.09 Å, which are very close to those of  $Pd_3LiO$ . The FE value is 2.11 eV while the HLG is 0.03 eV. In the ground state structure of  $Pd_3CoLiO$  having anti  $\pi$  bondings (see Fig. 2), LiO binds to the Co site. The Co-O bond distance is 1.71 Å, which is similar to the other atop site absorptions. The addition of a Pd atom to  $Pd_2CoLiO$  has little effect on the Li-O bond distance. In the quintet magnetic state, the BE of  $Pd_3CoLiO$  is 2.65 eV. The HLG is 0.50 eV while the FE of this structure is 3.59 eV. With FE of 3.36 eV, the spin moment of  $Pd_2Co_2LiO$  is 5  $\mu_B$ .

#### Lowest Energy Structures of $Pd_n Co_m Li_2 O$ ( $2 \leq n+m \leq 4$ )

The lowest lying energetic structures of

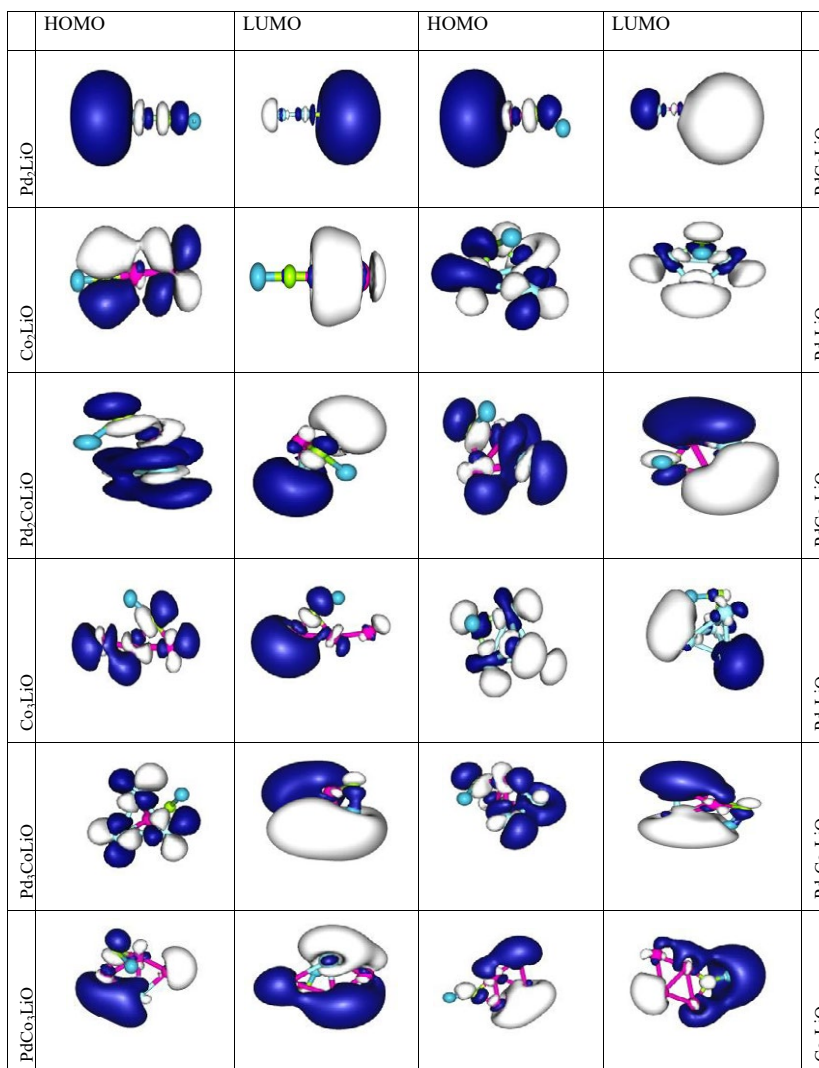


Fig. 2. The HOMO-LUMO density plots of Pd<sub>n</sub>Co<sub>m</sub>LiO Nanoparticles (2≤m+n≤4)

Table 1. The Electronic Properties of Pd<sub>n</sub>Co<sub>m</sub>LiO (2≤n+m≤4) Structures<sup>a</sup>

Nanoparticles	SYM	SM	BE*	BE**	FE	HLG
Pd <sub>2</sub> LiO	C <sub>s</sub>	3	2.07	2.76	2.05	0.42
PdCoLiO	C <sub>s</sub>	4	2.61	3.19	2.51	0.05
Co <sub>2</sub> LiO	C <sub>s</sub>	5	2.65	3.11	2.81	1.26
Pd <sub>3</sub> LiO	C <sub>s</sub>	1	2.36	2.92	3.78	0.50
Pd <sub>2</sub> CoLiO	C <sub>s</sub>	4	2.64	3.11	3.65	0.73
PdCo <sub>2</sub> LiO	C <sub>1</sub>	5	2.65	3.02	3.27	0.83
Co <sub>3</sub> LiO	C <sub>1</sub>	6	2.53	2.82	3.61	0.46
Pd <sub>4</sub> LiO	C <sub>1</sub>	3	2.33	2.81	2.11	0.03
Pd <sub>3</sub> CoLiO	C <sub>1</sub>	4	2.65	3.06	3.59	0.50
Pd <sub>2</sub> Co <sub>2</sub> LiO	C <sub>s</sub>	5	2.68	3.01	3.36	0.49
PdCo <sub>3</sub> LiO	C <sub>s</sub>	8	2.61	2.87	3.87	0.61
Co <sub>4</sub> LiO	C <sub>1</sub>	9	2.57	2.74	2.83	0.95

<sup>a</sup>SYM, Point Group Symmetry; SM, Spin Moment in μB; BE, Binding Energy in eV/atom; Fermi Energy, FE in eV; HLG, HOMO-LUMO Gap in eV

\*non-vdw corrected

\*\* vdw corrected

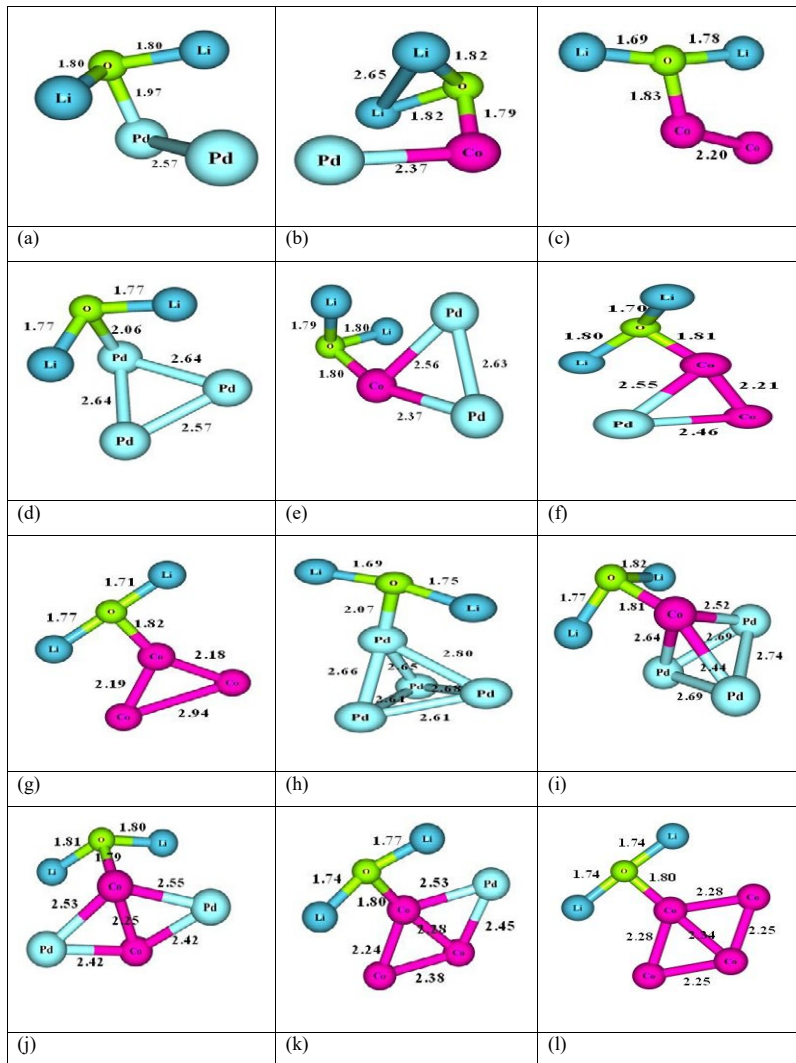


Fig. 3. The optimized structures of Pd<sub>n</sub>Co<sub>m</sub>Li<sub>2</sub>O Nanoparticles (2≤m+n≤4)

Table 2. The Electronic Properties of Pd<sub>n</sub>Co<sub>m</sub>Li<sub>2</sub>O (2≤n+m≤4) Structures<sup>a</sup>

Table 2 The Electronic Properties of Pd <sub>n</sub> Co <sub>m</sub> Li <sub>2</sub> O (2≤n+m≤4) Structures <sup>a</sup>						
Nanoparticles	SYM	SM	BE*	BE**	FE	HLG
Pd <sub>2</sub> Li <sub>2</sub> O	C <sub>s</sub>	0	2.48	3.03	1.93	0.77
PdCoLi <sub>2</sub> O	C <sub>s</sub>	3	2.66	3.12	1.25	1.02
Co <sub>2</sub> Li <sub>2</sub> O	C <sub>1</sub>	4	2.56	2.94	1.73	0.73
Pd <sub>3</sub> Li <sub>2</sub> O	C <sub>1</sub>	2	2.44	2.92	3.97	0.15
Pd <sub>2</sub> CoLi <sub>2</sub> O	C <sub>1</sub>	3	2.65	3.06	1.04	0.84
PdCo <sub>2</sub> Li <sub>2</sub> O	C <sub>1</sub>	4	2.58	2.92	2.98	0.46
Co <sub>3</sub> Li <sub>2</sub> O	C <sub>1</sub>	7	2.56	2.82	2.59	0.89
Pd <sub>4</sub> Li <sub>2</sub> O	C <sub>1</sub>	2	2.45	2.88	3.10	0.07
Pd <sub>3</sub> CoLi <sub>2</sub> O	C <sub>1</sub>	3	2.66	3.05	3.18	0.59
Pd <sub>2</sub> Co <sub>2</sub> Li <sub>2</sub> O	C <sub>1</sub>	6	2.69	3.01	1.76	0.57
PdCo <sub>3</sub> Li <sub>2</sub> O	C <sub>1</sub>	7	2.64	2.88	3.01	0.72
Co <sub>4</sub> Li <sub>2</sub> O	C <sub>s</sub>	8	2.60	2.77	2.71	0.66

<sup>a</sup> SYM, Point Group Symmetry; SM, Spin Moment in μ<sub>B</sub>; BE, Binding Energy in eV/atom.; FE, Fermi Energy in eV; HLG, HOMO-LUMO Gap in eV  
\*non-vdW corrected  
\*\* vdW corrected

$Pd_nCo_mLi_2O$  ( $2 \leq n+m \leq 4$ ) mixed metal oxides are shown in Fig. 3 and the density plots of HOMO and LUMO calculations are given in Fig. 4. The total spin moments, BEs, FEs and HLG of these nanoparticles are listed in Table 2. The BEs per atoms of these species is plotted in Fig. 6.

The  $Li_2O$  is, see Fig. 3a, adsorbed on  $Pd_2$  dimer molecularly at the top site where O is bonded to one of the Pd atoms. The BE of the lowest energy structure of  $Pd_2Li_2O$  is 2.48 eV. This structure, including  $\pi$  bonds has closed shell magnetic moment. The HLG energy of  $Pd_2Li_2O$  having  $C_s$  symmetry is 0.77 eV, while its FE is 1.93 eV. The ground state structure of the  $PdCoLi_2O$  is in the quartet magnetic state with

$C_s$  symmetry.  $Li_2O$  molecule is absorbed on the Co atom in this structure. The Li-O bond length is 1.82 Å in this structure while that bond length in  $PdCoLiO$  nanoparticle is 1.66 Å. The addition of the Li atom to  $LiO$  molecule at the PdCo cluster leads to expand Co-Pd distance by 0.1 Å. The HLG of the particle is 1.02 eV, whereas the FE is 1.25 eV. The BE of  $PdCoLi_2O$  is 2.66 eV. The Co-Co bond distance of the  $Co_2$  dimer after  $Li_2O$  adsorption became 2.20 Å, which is longer than that of  $Co_2LiO$  structure.

Furthermore, the Co-O bond length is 1.83 Å, while Li-O bond lengths in this structure (see Fig. 3c) are 1.69 and 1.78 Å. The HLG energy is 0.73 eV.

	HOMO	LUMO	HOMO	LUMO	
$Pd_2Li_2O$					$PdCoLi_2O$
$Co_2Li_2O$					$Pd_4Li_2O$
$Pd_2CoLi_2O$					$Pd_2Co_2Li_2O$
$Co_3Li_2O$					$Pd_4Co_2Li_2O$
$Pd_3CoLi_2O$					$PdCo_3Li_2O$
$PdCo_3Li_2O$					$Co_4Li_2O$

Fig. 4. The HOMO-LUMO density plots of  $Pd_nCo_mLi_2O$  Nanoparticles ( $2 \leq m+n \leq 4$ )

The BE per atom of this structure, which has 4  $\mu_B$  magnetic moment, is 2.56 eV.

$Pd_3Li_2O$  has a triangular unit like  $Pd_3LiO$ . The magnetic state of this structure is a triplet. The BE of the cluster is 0.04 eV less than that of  $Pd_2Li_2O$ . The adsorption of  $Li_2O$  is again on a top site. This type of adsorption is also observed for all studied  $Pd_nCo_mLi_2O$  nanoparticles. Furthermore, the HLG energy of this structure is 0.15 eV. As one of the Pd atoms replaces with a Co atom, the BE of the lowest energy structure of the  $Pd_2CoLi_2O$  becomes 2.65 eV, where O binds to the Co atom. The FE of this structure is 1.04 eV, while the HLG is 0.84 eV. The Co-Pd distances are 2.56 and 2.37 Å and the Co-O bond length is 1.80 Å, which is longer than the Co-O bond length of  $Pd_2CoLiO$ . The BE per atom of  $PdCo_2Li_2O$  is 2.58 eV. The lowest energy morphology is similar to that of  $Pd_2CoLi_2O$ .  $Li_2O$  is adsorbed on the Co side as usual. The magnetic state of  $PdCo_2Li_2O$  is quintet. The Co-Co bond length of this cluster is 2.21 Å, which is nearly the same as that of  $Co_2Li_2O$  cluster. The HLG of  $Co_3Li_2O$  is calculated as 0.89 eV while the FE is 2.59 eV. The BE of  $Co_3Li_2O$  is 0.02 eV less than that of  $PdCo_2Li_2O$ .

The Co-O bond length is also very similar to that of the previous cluster. Li-O bond lengths are 1.71 Å and 1.77 Å. The geometries of  $Co_3$  unit in  $Co_3LiO$  and  $Co_3Li_2O$  are highly different.

The ground state structure of  $Pd_4Li_2O$  has distorted tetrahedral metallic unit in the triplet magnetic state with the average Pd-Pd bond distance of 2.72 Å, which is longer than that of the  $Pd_3Li_2O$ . The BE of this structure is, see Table 2, 2.45 eV with Pd-O bond length of 2.07 Å, while FE is 3.10 eV. The HLG is calculated as 0.07 eV. Placing a Co atom instead of a Pd atom leads to stretch the bonds between Li and O, which are 1.77 Å and 1.82 Å in  $Pd_3CoLi_2O$ , while they are 1.69 Å and 1.75 Å in  $Pd_4Li_2O$ . The Co-O bond length in  $Pd_3CoLi_2O$  is nearly the same with that of  $Pd_2CoLi_2O$ . Moreover, the distorted tetrahedral configuration of metallic unit is kept in  $Pd_3CoLi_2O$  cluster. The BE per atom for this structure is calculated as 2.66 eV with a FE of 3.18 eV, while the HLG is calculated as 0.59 eV. The magnetic moment of the structure is found as 3  $\mu_B$ . As Co doping increases by keeping a number of metallic atoms fixed, there is no important change for Li-O and Co-O bond lengths. However,

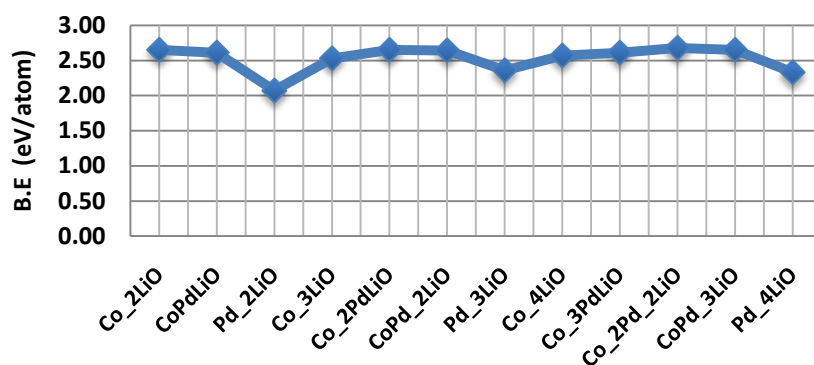


Fig. 5. The Binding Energies (BEs) per atom of  $Pd_nCo_mLiO$  Nanoparticles ( $2 \leq m+n \leq 4$ )

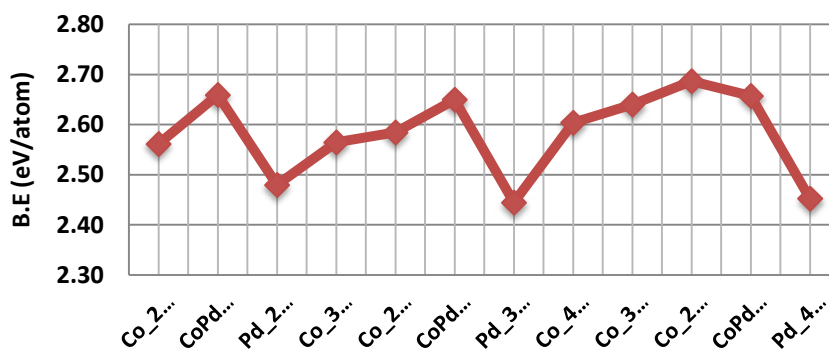


Fig. 6. The Binding Energies (BEs) per atom of  $Pd_nCo_mLi_2O$  Nanoparticles ( $2 \leq m+n \leq 4$ )

the tetrahedral metallic unit becomes an out of plane rhombus for Pd<sub>2</sub>Co<sub>2</sub>Li<sub>2</sub>O. Furthermore, Li<sub>2</sub>O molecule binds to the top site of a Co atom where the Co-O bond length is 1.79 Å, while this bond length in the Pd<sub>2</sub>Co<sub>2</sub>LiO is 1.90 Å with bridge site adsorption. Moreover, the average Co-Pd bond distance is 2.48 Å and the Co-Co bond distance is 2.25 Å in this structure (see Fig. 3j). The HLG is 0.57 eV, while FE is 1.76 eV. The BE of the structure is 2.69 eV in the quintet magnetic state. When one of the Pd atoms of Pd<sub>2</sub>Co<sub>2</sub>Li<sub>2</sub>O is changed with a Co atom, the rhombic morphology does not change. In the ground state structure of PdCo<sub>3</sub>Li<sub>2</sub>O, the BE is calculated as 2.64 eV, where Li<sub>2</sub>O is adsorbed on the Co side again. The Co-Co bond distances are 2.24 Å and 2.38 Å (see Fig. 3k) and the Co-Pd bond distances are 2.45 Å and 2.53 Å. The magnetic moment of this structure is 7 μ<sub>B</sub>, while the FE is 3.01 eV. The HLG energy of Pd<sub>3</sub>CoLi<sub>2</sub>O is 0.59 eV. The BE per atom of Co<sub>4</sub>Li<sub>2</sub>O cluster with C<sub>s</sub> symmetry is 2.60 eV/atom. Its magnetic state is 8 μ<sub>B</sub>. The replacement of the single Pd atom of PdCo<sub>3</sub>Li<sub>2</sub>O structure by a Co atom has little effect on Li-O bond length. The Co-Co bond distance of 2.28 Å is 0.10 Å longer than the corresponding distances of Co<sub>3</sub>Li<sub>2</sub>O structure. It can be concluded that the addition of a new Co atom to Co<sub>3</sub>LiO leads to an expansion in the Co-Co distances. Moreover, the FE of this structure is 2.71 eV, whereas the HLG is 0.66 eV

#### Stability and Electronic Properties

The BEs of the clusters can be used as a measure for their thermodynamic stabilities. Accordingly, to predict the relative stabilities of the Pd<sub>n</sub>Co<sub>m</sub>Li<sub>x</sub>O structures, the BEs per atom are calculated, tabulated in Table 1 and Table 2 and plotted in Fig. 5 and Fig. 6.

The BEs per atom can be obtained in the following way:

$$BE = \frac{-E[Pd_mCo_nLi_xO] + mE[Co] + nE[Pd] + xE[Li] + E[O]}{n + m + x + 1} \quad (1)$$

Where E[\*] is the total energy of Co, Pd, Li and O atoms respectively for 2 ≤ n+m ≤ 4 and x=1 or 2. While the BEs of the lowest energy structures of Pd<sub>n</sub>Co<sub>m</sub>LiO vary between 2.07 eV and 2.68 eV, those of Pd<sub>n</sub>Co<sub>m</sub>Li<sub>2</sub>O changes from 2.44 eV to 2.69 eV. On the other hand, for a comparison of BEs values in terms of London dispersion effect, we

have calculated the vdW corrected BE values, as listed in Table 1 and Table 2.

Similar trends are observed in vdW corrected BE. The BE values shift approximately 0.5 eV when compared to the non-vdW corrected calculations.

The HOMO can be defined as an ability of the structure to give an electron, while the energy of the LUMO is an ability of the structure to accept an electron. The higher the HOMO energy, the higher the ability to give an electron, and the lower the LUMO energy, the higher is the tendency to accept an electron. A large HLG can be defined as a significant requirement for chemical stability to a certain degree. The HLG values are listed in Table 1 and Table 2. According to the HLG results, the studied structures indicate conductor properties since the HLG values range from 0.05 eV to 1.26 eV, which are chemically very active. The HLG and BE analyses show that the smallest stability or highest activity belongs to the Pd<sub>4</sub>Li<sub>2</sub>O nanoparticle.

The charge transfer between PdCo and Li<sub>x</sub>O has been analyzed based on Mulliken charge analyses. The charge calculations of each atom of PdCoLi<sub>x</sub>O structures are listed in Table S1 and S2. Generally, in the structures, for cobalt atoms, it loses their electrons to mostly O atom and Pd atoms almost keep their charges, but in the absence of Co atoms, Pd loses their electrons to mostly O atom. Li atoms in the structures gain ignorable charges. This is supported by Homo-Lumo plot. The intensity of the charge transformation around Co atoms is high but the intensity of the charge transformation around Li atoms is low.

#### CONCLUSION

In terms of electronic, structural and magnetic properties, Pd<sub>n</sub>Co<sub>m</sub>Li<sub>x</sub>O (2 ≤ n+m ≤ 4 and x=1 or 2) nanoparticles were studied by means of the DFT method. The effects of LiO and Li<sub>2</sub>O adsorptions on the lowest energetic structure of the small bimetallic Pd-Co nanoparticles were examined. Results show that LiO molecule is adsorbed on atop or bridge sites of small Pd-Co bimetallic clusters while Li<sub>2</sub>O molecule prefers to be adsorbed on atop sites. This information may be important for determining active site in catalytic reaction to design effective catalytic material. We do not also observe any hollow site adsorption in this study. The topology of the bare Pd-Co bimetallic nanoparticles generally does not change due to the Li<sub>x</sub>O adsorptions. Li<sub>x</sub>O (x=1 and 2) molecules tend to bind Co atoms instead of Pd atoms. The



structures having an equal or nearly equal number of Pd and Co atoms possess the highest BEs. The charge analyses and HOMO-LUMO density plot reveal that Co atoms are very active in charge transformation. This may be due to the unpaired electrons of Co atoms. In addition, According to the HLG analyses, the studied nanoparticles show conductive properties.

#### CONFLICT OF INTEREST

The authors declare that there is no conflict of interests regarding the publication of this manuscript.

#### REFERENCES

1. A. Dolatkah, P. Jani, L. D. Wilson, *Langmuir*, 2018).
2. M. L. Weichman, S. Debnath, J. T. Kelly, S. Gewinner, W. Schöllkopf, D. M. Neumark, K. R. Asmis, *Topics in Catalysis*, 61 92 (2018).
3. M. Ovais, A. T. Khalil, N. U. Islam, I. Ahmad, M. Ayaz, M. Saravanan, Z. K. Shinwari, S. Mukherjee, *Applied microbiology and biotechnology*, 1 (2018).
4. D. Sarker, S. Bhattacharya, H. Kumar, P. Srivastava, S. Ghosh, *Scientific reports*, 8 1040 (2018).
5. D. Sharma, M. I. Sabela, S. Kanchi, K. Bisetty, A. A. Skelton, B. Honarparvar, *Journal of Electroanalytical Chemistry*, 808 160 (2018).
6. A. Abbasi, J. J. Sardroodi, *Applied Surface Science*, 436 27 (2018).
7. H. Eskalen, S. Kerli, Ş. Özgan, in *Cobalt, InTech*, 2017.
8. Y. Bao, W.-D. Oh, T.-T. Lim, R. Wang, R. D. Webster, X. Hu, *Chemical Engineering Journal*, 353 69 (2018).
9. M. Aslan, R. L. Johnston, *The European Physical Journal B*, 91 120 (2018).
10. M. Aslan, R. L. Johnston, *The European Physical Journal B*, 91 138 (2018).
11. W. Zhang, H. Zhao, L. Wang, *The Journal of Physical Chemistry B*, 108 2140 (2004).
12. F. B. Noronha, M. Schmal, C. Nicot, B. Moraweck, R. Frety, *Journal of Catalysis*, 168 42 (1997).
13. S. Bischoff, A. Weigt, K. Fujimoto, B. Lücke, *Journal of Molecular Catalysis A: Chemical*, 95 259 (1995).
14. M. Heemeier, A. F. Carlsson, M. Naschitzki, M. Schmal, M. Bäumer, H. J. Freund, *Angewandte Chemie International Edition*, 41 4073 (2002).
15. S. Maheswari, S. Karthikeyan, P. Murugan, P. Sridhar, S. Pitchumani, *Physical Chemistry Chemical Physics*, 14 9683 (2012).
16. H. Cantera-López, J. M. Montejano-Carrizales, F. Aguilera-Granja, J. L. Morán-López, *Eur. Phys. J. D*, 57 61 (2010).
17. S. H. Oh, R. Black, E. Pomerantseva, J.-H. Lee, L. F. Nazar, *Nat Chem*, 4 1004 (2012).
18. W. G. Hardin, D. A. Slanac, X. Wang, S. Dai, K. P. Johnston, K. J. Stevenson, *The Journal of Physical Chemistry Letters*, 4 1254 (2013).
19. B. Cui, H. Lin, J.-B. Li, X. Li, J. Yang, J. Tao, *Advanced Functional Materials*, 18 1440 (2008).
20. L. Leng, J. Li, X. Zeng, H. Song, T. Shu, H. Wang, S. Liao, *Journal of Power Sources*, 337 173 (2017).
21. M. Sevim, C. Francia, J. Amici, S. Vankova, T. Şener, Ö. Metin, *Journal of Alloys and Compounds*, 683 231 (2016).
22. A. D. Becke, *Physical Review A*, 38 3098 (1988).
23. C. Lee, W. Yang, R. G. Parr, *Physical Review B*, 37 785 (1988).
24. M. Valiev, E. J. Bylaska, N. Govind, K. Kowalski, T. P. Straatsma, H. J. Van Dam, D. Wang, J. Nieplocha, E. Apra, T. L. Windus, *Computer Physics Communications*, 181 1477 (2010).
25. M. M. Hurley, L. F. Pacios, P. A. Christiansen, R. B. Ross, W. C. Ermler, *The Journal of Chemical Physics*, 84 6840 (1986).
26. M. Valiev, E. J. Bylaska, N. Govind, K. Kowalski, T. P. Straatsma, H. J. J. Van Dam, D. Wang, J. Nieplocha, E. Apra, T. L. Windus, W. A. de Jong, *Computer Physics Communications*, 181 1477 (2010).
27. G. A. DiLabio, M. Koleini, E. Torres, *Theoretical Chemistry Accounts*, 132 1389 (2013).
28. D. E. Gray, *American institute of physics handbook*, 1972.
29. B. R. Sahu, G. Maofa, L. Kleinman, *Physical Review B*, 67 115420 (2003).